energies

MDPI

Article

Investigation Concerning the Excitation Loss of Synchronous Generators in a Stand-Alone Ship Power Plant

Dariusz Tarnapowicz *, Sergey German-Galkin and Marek Staude

Faculty of Mechatronics and Electrical Engineering, Maritime University of Szczecin, 70-500 Szczecin, Poland; s.german-galkin@am.szczecin.pl (S.G.-G.); m.staude@am.szczecin.pl (M.S.)
* Correspondence: d.tarnapowicz@am.szczecin.pl

Abstract: The protection systems of ship generators enable them to eliminate potential failures that pose a significant threat to the safety of the crew and the use of the ship. However, due to the fact that marine classification societies do not require the protection of generators against the loss of excitation, such protection is only used sporadically. This article presents an LOE (loss of excitation) analysis of ship generators that operate in parallel. This analysis is supported by simulations and experimental research. The test results show that the positions of the operating points of each generator are interrelated, and changes in the excitation of one (damaged) generator cause automatic changes in the excitation, as well as changes in electromagnetic and energy processes, in the second (efficient) generator. An LOE in one generator causes a dangerous increase in armature currents in both generators. The results of this study prove that the lack of LOE protection at lower levels of excitement in one of the generators causes (by activating the required protection) the efficient generator to be switched off first. The main conclusion of this article is that the introduction of the use of security measures against LOE should be obligatory and legally required.

Keywords: stand-alone power plant; loss of excitation; asynchronous operation of synchronous generators

Citation: Tarnapowicz, D.; German-Galkin, S.; Staude, M. Investigation Concerning the Excitation Loss of Synchronous Generators in a Stand-Alone Ship Power Plant. *Energies* **2021**, *14*, 2828. https://doi.org/10.3390/en14102828

Academic Editor: Cristina González-Morán

Received: 20 April 2021
Accepted: 12 May 2021
Published: 14 May 2021

1. Introduction

The power system is the most important system in a watercraft. It affects the watercraft's life cycle as an autonomous unit. In order to ensure the safe and efficient use of the ship, it is necessary to ensure that the electricity generated is of high quality. The complexity of this task results from the use of multi-generator power plants and the need to ensure the parallel operation of electric energy sources [1].

Modern marine power systems have a large number of automation systems that ensure the parallel operation of marine generating sets [1,2]. However, there are many emergency situations. They occur due to the poor quality of the parallel operation of the power sources. The reasons for this situation are the incomplete examination of all electromagnetic and energy processes, imperfections in the automation systems, and insufficiently qualified operating personnel. One of the poorly examined problems concerning the parallel operation of marine generating sets is the loss of stability in a ship's power system.

Commonly, the main elements of ship power systems are synchronous generators (SGs) that use electromagnetic excitation, which are usually powered by combustion engines (AEs—auxiliary engines). A ship power plant consists of (at least) two generating sets [3,4] (usually three or more diesel–generator sets (D-G)) (Figure 1). The specificity of a ship's power grid in relation to the classic (common) onshore grid is connected with the power of some individual receivers with respect to the power of the generators. This is a so-called "soft" ("flexible") grid. It is also important that D-G sets operate in parallel on a common receiving grid. The parallel operation of D-G sets is related to the power demand, but above all, it is to ensure the safe operation of the ship. Similar power systems—

where the parallel operation of two D-G sets is sometimes necessary—are used on land (autonomous systems) [5–8].

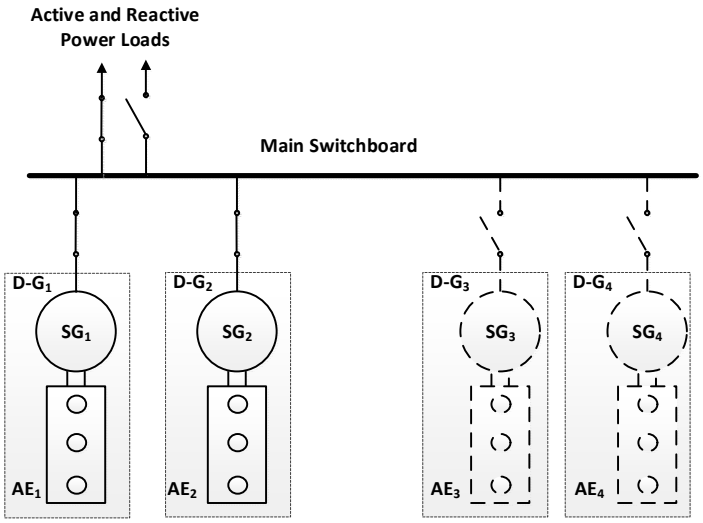

Figure 1. Simplified diagram of a ship power system.

Synchronous generators are exposed to many different types of defects and abnormal operating conditions. The occurrence of abnormal states in the generators can have catastrophic consequences. Generator failures imply high costs for shipowners. They result not only from the need to repair or replace a damaged machine, but also from the inability to operate the ship. Therefore, in the event of a failure, the protective systems must be selective and fast in order to isolate the machine from the system immediately.

Disturbances in the operation of synchronous generators may be external or internal. External disturbances of generators include disturbances related to the power system or the generator's drive [8]. Internal disturbances include short circuits generated in the stator and rotor windings, as well as damages covering the whole excitation system. The most common causes of all types of disturbances include aging of the insulation, mechanical damage to the insulation, construction defects, and connection failures. Dangers in the operation of generators include voltage increases at the generator's terminals, thermal overload of the windings, external short circuits, individual short circuits in the winding, load asymmetry, motor operation, loss of excitation, and mechanical disturbances. Some disturbances can only be signaled, while others cause disconnection of the generator.

The requirements for the rules and regulations for ship classification that were published by classification societies are based on the applicable standards for ships published by the IEC (International Electrotechnical Commission) [9].

In accordance with the requirements of classification societies, ship generators must be protected from four parameters [10–13]:

- Overloads;
- Short circuits;
- Inverse power;
- Voltage (undervoltage protection).

LOE protection is not required by ship classification societies.

The static and dynamic instability of SGs (operating in a rigid power grid) has been thoroughly examined and widely discussed in the literature. One of the common causes of static instability in SGs is the loss of excitation [14–18].

The most common cause of LOE in marine generators is the incorrect operation of the voltage regulator and damage to the diode in the rotating rectifier bridge of the SG magnetizer.

The effects of the loss of excitation in autonomous power plants, such as ship power plants, may pose a significant threat to the safety of the crew and the exploitation of the

ship. The loss of excitation and (consequently) the loss of synchronism by the generator will have an impact on the power system and the generating set in the following ways [19]:

- The absorption of reactive power (to a large extent);
- The heating of the generator's rotor;
- The libration of the set of generators;
- The probable formation of resonant overvoltage.

A family of characteristics called the V-curve [20,21] is used for the evaluation of the static stability of an SG (operating in parallel with the grid with a constant frequency f and voltage U). V-curves for four values of the active output power P of a generator are shown in relative values in Figure 2. They represent the dependence of the current I at the generator output on the excitation current $I_{ex}(I = f(I_{ex}))$. The minimum values of the currents I are presented on the CD curve. They represent the SG's control characteristics: $\cos \Phi = 1$.

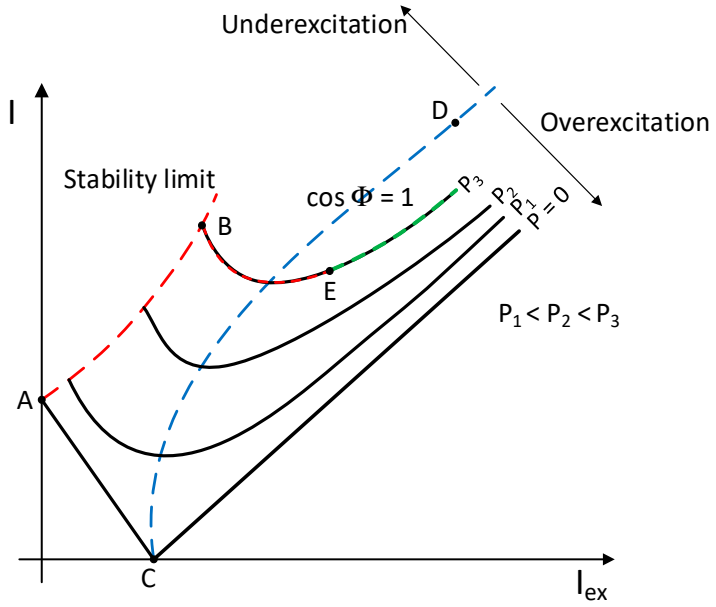

Figure 2. V-curve.

To the right of the CD curve, the generator's load is active–inductive. The load current magnetizes the generators and its emf increases. In the points on the left side of the CD curve, the generator's load is active–capacitive. The load current demagnetizes the generator and its emf decreases. The AB curve is a limit of the static stability at which the generator "loses the ability" to maintain synchronous rotation in an independent way, and it falls out of synchronism (goes into an asynchronous mode of operation).

The problem of LOE (loss of excitation) in the case of the parallel operation of a synchronous generator with a rigid grid has been widely presented in the literature, but in the case of ship power plants (as well as onshore autonomous power plants), where we deal with the parallel operation of two or more generators that are working on a single load, it has not been discussed.

A methodology was developed to analyze the electromagnetic and energy processes in a system of two ship generator sets operating on a common load. Using this methodology, based on the geometric relations of the vector diagrams, the electromagnetic and energetic characteristics of the system were calculated, and the parameters for the transition of the units to the asynchronous operation regime were determined. A model of the system was developed in the Matlab-Simulink environment, and experimental tests were carried out in a laboratory.

The symptoms and effects of the loss of excitation of a damaged generator and their impact on the operation of the second (undamaged) generator are presented. As a result

of analytical, simulated, and experimental tests, it was proved that a partial LOE and a complete LOE can lead to the failure of a ship's power plant system, and the generator protections that are currently used on ships are not effective against such threats.

2. Analysis of the SG Excitation Loss in the Parallel Operation of Generating Sets

A different physical picture of the LOE in an SG is observed in autonomous electric grids—in particular, in ship grids. In such grids, two generators with the same power very often operate on a common load (Figure 1). In such systems, the positions of the operating points of each generator on the "V-curve" (Figure 2) are interconnected, and a change in the excitation current of one generator results in an automatic change in the excitation current of the second generator.

The mathematical description of the system with two generators operating in parallel for a common load in the x, y coordinate system (rotating synchronously with the rotating fields SG1 and SG2) can be presented in the following way [22]:

$$\begin{array}{l} \overline{E}_1(t) = \overline{U}_L(t) + L_1\frac{d\overline{I}_1(t)}{dt} + r_1\overline{I}_1(t)_1 + x_1\overline{I}_1(t), \\ \overline{E}_2 = \overline{U}_L(t) + L_2\frac{d\overline{I}_2(t)}{dt} + r_2\overline{I}_2(t) + x_2\overline{I}_2(t), \\ \overline{I}_L(t) = \overline{I}_1(t) + \overline{I}_2(t). \end{array} \quad (1)$$

where:

$\overline{U}_L, \overline{I}_L = \overline{I}_1 + \overline{I}_2$—load voltage and current and armature currents for the first and second generator;

r_1, r_2—resistance of the armature windings (first and second generator);

L_1, L_2—inductance of the armature windings (first and second generator);

$x_1 = \omega L_1, x_2 = \omega L_2$—reactance of the armature windings (first and second generator);

$\overline{E}_1, \overline{E}_2$—emf of the first and second generator.

In the synchronous state, the system of Equation (1) transforms into the form:

$$\begin{array}{l} \overline{E}_1 = \overline{U}_L + r_1\overline{I}_1 + x_1\overline{I}_1, \\ \overline{E}_2 = \overline{U}_L + r_2\overline{I}_2 + x_2\overline{I}_2, \\ \overline{I}_L = \overline{I}_1 + \overline{I}_2. \end{array} \quad (2)$$

The electromagnetic processes occurring in a synchronous generator when operated autonomously or in parallel with the grid are traditionally studied in the d, q coordinate system, which is associated with the excitation field and EMS of the generator. In the study of two generators operating on a common load, it is necessary to depart from the traditional approach and consider the electromagnetic processes in a coordinate system associated with a common load. In this article, this coordinate system is marked as x, y.

In the x, y coordinate system, Equation (2) can be presented as:

$$\begin{array}{l} E_{1x} = 0 + r_1 I_{1x} - x_1 I_{1y}, \\ E_{1y} = U_L + r_1 I_{1y} + x_1 I_{1x}, \\ E_{2x} = 0 + r_2 I_{2x} - x_2 I_{2y}, \\ E_{2y} = U_L + r_2 I_{2y} + x_2 I_{2x}, \\ I_{Lx} = I_{1x} + I_{2x}, \\ I_{Ly} = I_{1y} + I_{2y}. \end{array} \quad (3)$$

The analysis of the mutual influence of the generators operating in parallel on the common load was conducted with the use of the systems of Equations (2) and (3) and the vector diagram of the whole generating system (Figure 3). Each generator set contains a closed stabilization system of speed and voltage.

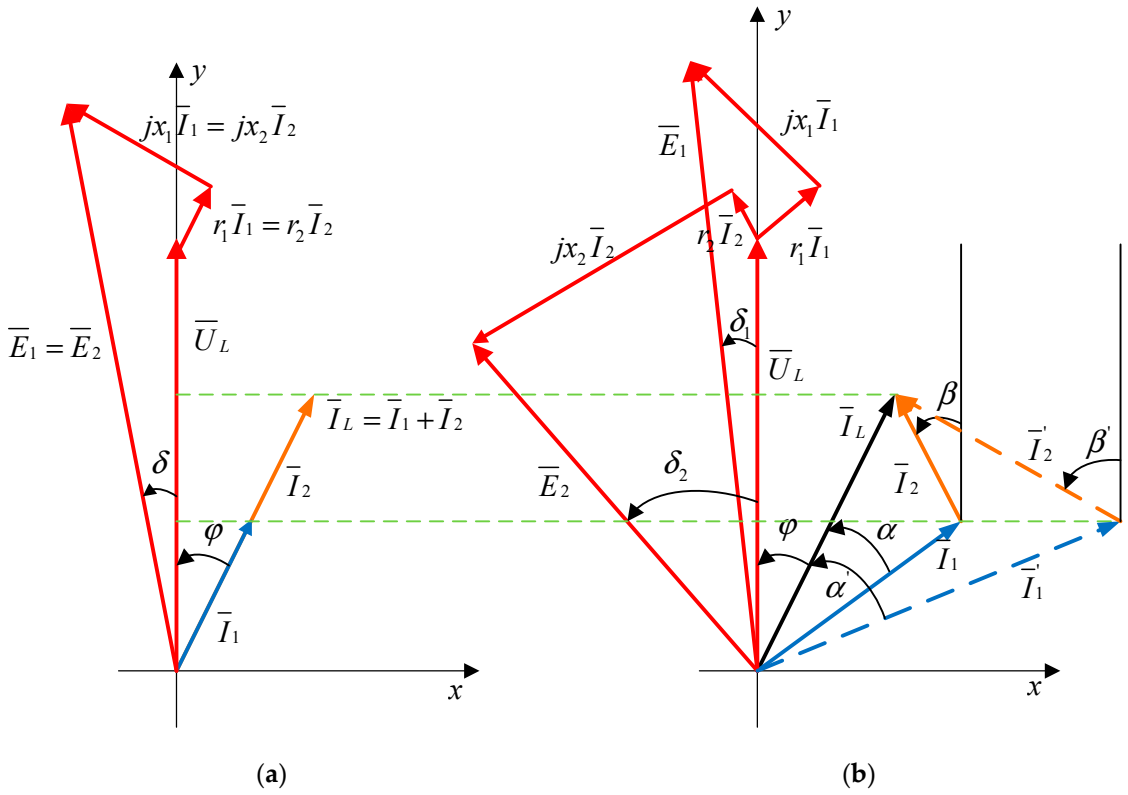

Figure 3. Vector diagrams of generators operating in parallel: (**a**) in the symmetrical operation mode; (**b**) in the asymmetrical operation mode.

The following symbols are used in the vector diagram:

φ—phase shift between the load current and voltage;

δ_1, δ_2—load angles for the first and second generators;

α, α'—angle of mismatch (phase shift between the first generator's current and load current);

β, β'—angle of mismatch (phase shift between the second generator's current and load voltage).

The vector diagram shows two cases. In the first case (Figure 3a), the parameters of the voltage and speed regulators of both generators are the same, and the active and reactive power (currents) transferred by the generators to the load and emf of the generators is (are) the same. In the second case (Figure 3b), the load voltage and current remain unchanged, the reactive current of the second generator is lower than that of the first generator, and the active currents of the generators remain equal.

The vector diagram of the symmetrically operating generators (Figure 3a) corresponds to point E on the "V-curve" (Figure 2). The appearance of a difference $\Delta\bar{E} = \bar{E}_1 - \bar{E}_2$ leads to the fact that the operating point of the first generator shifts to the right of point E, and the operating point of the second generator shifts to the left of point E. This shift causes an increase in $\Delta\bar{E}$, which leads to an even greater discrepancy in the operating points of the generators. Therefore, a slight asymmetry in the excitation channels of the generators leads to the appearance of a positive feedback in the system, which brings the operating point of one generator to the limit of static stability (AB) (Figure 2). The vector diagram (Figure 3b) clearly shows that while the total load current remains unchanged ($\bar{I}_L$), the currents change ($\bar{I}_2$ $\bar{I}_1$). Simultaneously, the current inductive component ($\bar{I}_1$) increases; the current inductive component ($\bar{I}_2$) initially decreases, and then the capacitive component appears and increases.

The process of changing the values of the currents ($\bar{I}_1$ and $\bar{I}_2$) and mismatch angles (α and β) takes place over time. In the analysis, it is assumed that the angle of mismatch (α) grows proportionally to time and that it is an independent argument. The angle α varies

from the value $\alpha = \phi$ to the value $\alpha = \alpha_{\lim}$, which can be determined on the basis of the vector diagram, assuming that the angle $\beta = \delta_2$ is equal to 90°.

The equations for calculating the generators' currents with the values obtained from the geometrical relationships [23] (vector diagram—Figure 3) are presented below.

$$\begin{aligned} I_{1y} &= kI_L \cos\varphi, \\ I_{2y} &= (1-k) I_L \cos\varphi, \\ I_{1x} &= kI_L \cos\varphi \cdot tg(\varphi + \alpha), \\ I_{2x} &= I_L \sin\varphi - (1-k) I_L \cos\varphi \cdot tg(\varphi + \alpha), \\ I_1 &= \sqrt{I_{1x}^2 + I_{1y}^2}, \\ I_2 &= \sqrt{I_{2x}^2 + I_{2y}^2}. \end{aligned} \tag{4}$$

where:

I_{1y}, I_{2y}—active components of the armature currents (first and second generator);
I_{1x}, I_{2x}—reactive components of the armature currents (first and second generator);
k—load distribution coefficient between the generators.

The load factor k varies depending on the distribution of the active load between the generators. Further examinations were conducted with the same active load distribution between the generators of $k = 0.5$.

In this case, the active powers of the load and generators are determined from the equations:

$$\begin{aligned} P_{1L} &= 1.5 U_L I_L \cos\varphi; \\ P_1 &= P_2 = 0.75 U_L I_L \cos\varphi. \end{aligned} \tag{5}$$

In order to visualize the analysis that was conducted, calculations were performed for an SG, the parameters of which are presented in Table 1. The parameters of the generator (in Table 1) were read from the rating plate of the generator used in the experimental tests (generator type: ELMOR GCf 74).

Table 1. SG parameters used in the tests.

S kVA	U V	I A	f Hz	n rpm	p	U_{ex} V	I_{ex} A	R Ω	L_s H
20	400	29	50	1500	2	50	8.3	1	0.012

In accordance with Equation (4), for $k = 0.5$, the dependencies of the SG's reactive currents I_{1x} and I_{2x} (Figure 4) and apparent currents I_1 and I_2 (Figure 5) on the angle $(\alpha + \phi)$ for the set value of the active power were determined.

The values of the load angles δ_1, δ_2 and emf of the generators E_1, E_2 were determined on the basis of Equation (3) and the vector diagram (Figure 3b).

$$\begin{aligned} \delta_1 &= arctg\tfrac{-E_{1x}}{E_{1y}} = arctg\tfrac{x_1 I_{1y} - r_1 I_{1x}}{U_L + x_1 I_{1x} + r_1 I_{1y}}; \\ E_1 &= \sqrt{\left(U_L + x_1 I_{1x} + r_1 I_{1y}\right)^2 + \left(x_1 I_{1y} - r_1 I_{1x}\right)^2}; \\ \delta_2 &= arctg\tfrac{-E_{2x}}{E_{2y}} = arctg\tfrac{x_2 I_{2y} - r_2 I_{2x}}{U_L + x_2 I_{2x} + R_2 I_{2y}}; \\ E_2 &= \sqrt{\left(U_L + x_2 I_{2x} + r_2 I_{2y}\right)^2 + \left(x_2 I_{2y} - r_2 I_{2x}\right)^2}. \end{aligned} \tag{6}$$

Figure 6 presents the course of the load angle δ_2 of the SG_2 generator. The total loss of excitation for SG_2 will occur at $\delta_2 = 1.57$ rad.

Figure 7 shows the dependence of the emf of SG_1 and SG_2 (E_1 and E_2) on the angle $\phi + \alpha$. It indicates that the emf limit value at $E_2 = E_{2gr}$ corresponds to the angle $\alpha = \alpha_{gr} = 1.36 - \phi$.

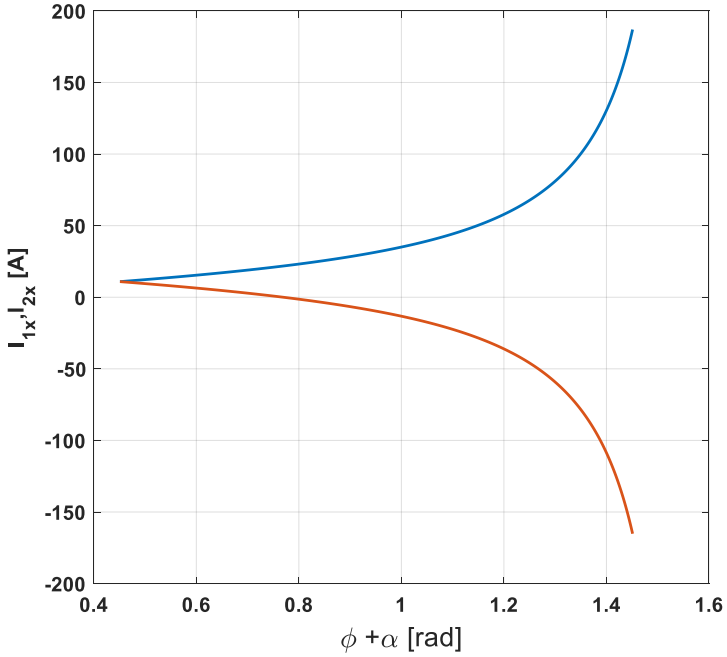

Figure 4. The dependence of the reactive currents I_{1x} and I_{2x} of the generators on the phase shift between the current of the first generator and the load voltage ($\phi + \alpha$).

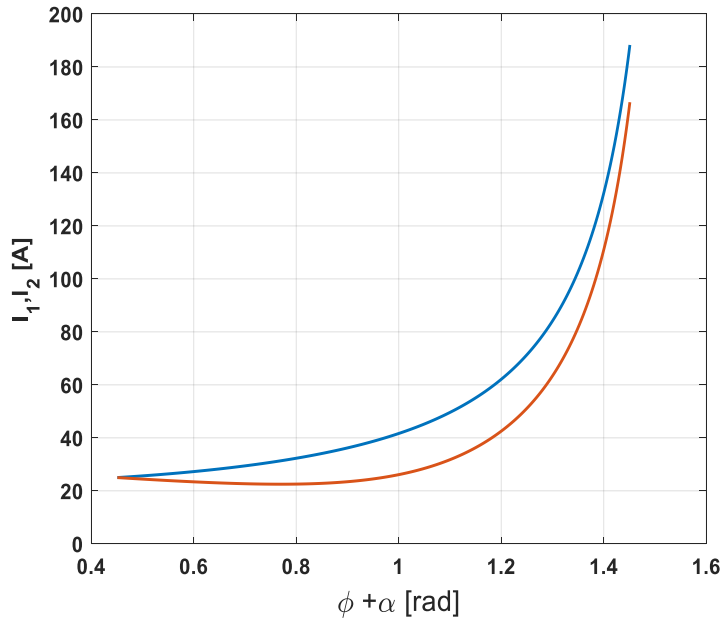

Figure 5. The dependence of apparent currents I_1 and I_2 of the generators on the phase shift between the current of the first generator and the load voltage ($\phi + \alpha$).

In the case of the occurrence of reactive currents, the reactive power in the system of two parallel generator sets is determined on the basis of the vector diagram with the use of the following equations:

$$\begin{aligned} Q_1 &= 1.5U_L I_1 \sin(\varphi + \alpha) = 1.5U_L I_{1x}; \\ Q_2 &= 1.5U_L I_2 \sin(\varphi + \beta) = 1.5U_L I_{2x}. \end{aligned} \tag{7}$$

where:

$$\beta = arctg\frac{x_2 I_{2x} + r_2 I_{2y}}{x_2 I_{2y}}$$

Figure 8 presents the dependence of the reactive power of generators Q_1 and Q_2 on the angle $\phi + \alpha$. According to the Equations (3) and (4), the appearance of asymmetry in the voltage regulators (loss of excitation for SG_2) causes a change in the reactive power of both generators. These changes continue to the value $\alpha = \alpha_{lim} = 1.36 - \phi$, at which the second generator loses synchronism (on the AB line (Figure 2)). It should be noted that the active powers of the generators in the synchronous operation mode remain constant and equal (Equation (2)).

The waveforms of the reactive power of Q_1 and Q_2 are similar to the waveforms of the reactive currents of the armature (I_{1x} and I_{2x} for SG_1 and SG_2 (Figure 4)).

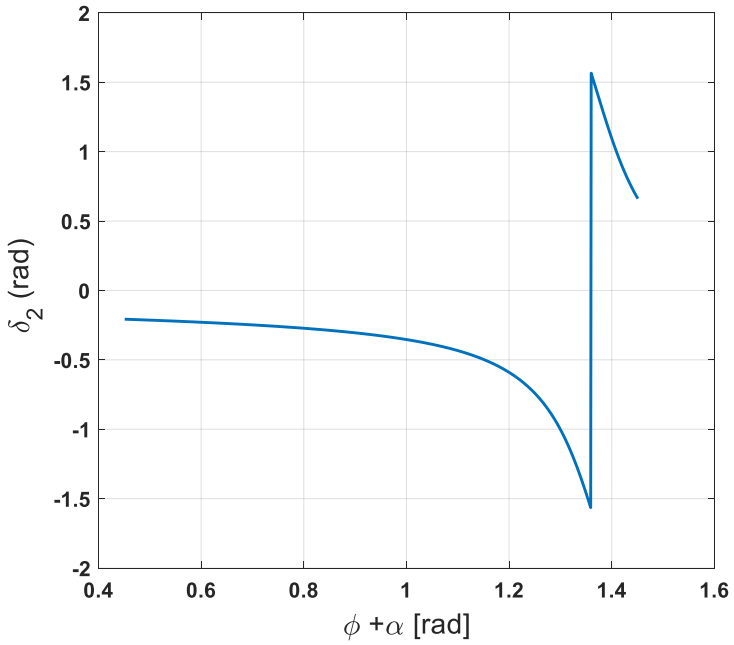

Figure 6. The dependence of the load angle δ_2 on the angle ($\phi + \alpha$).

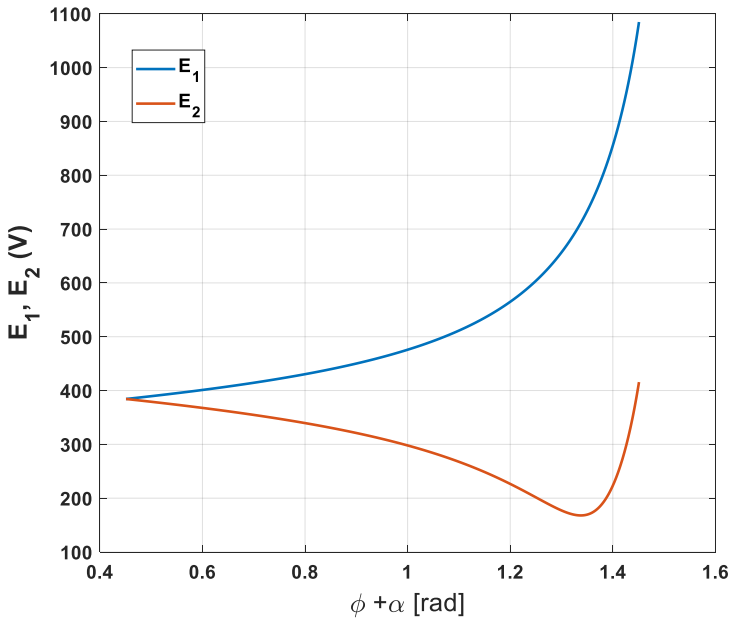

Figure 7. The dependencies of generators E_1 and E_2 on the angle $\phi + \alpha$.

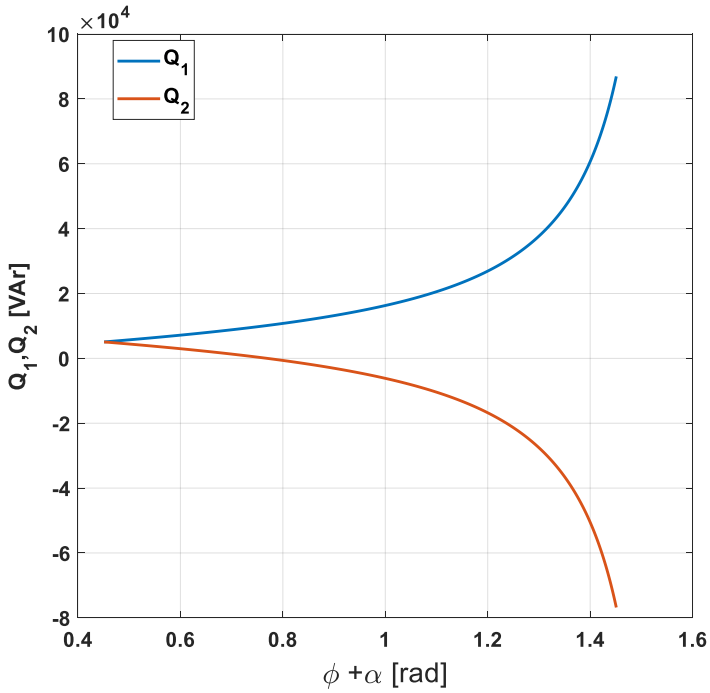

Figure 8. The dependence of the reactive power of generators Q_1 and Q_2 on the angle $\phi + \alpha$.

3. Simulation Results

In order to check the above analysis, simulation tests were conducted for a marine power plant system with synchronous generators with electromagnetic excitation (Figure 1). The parameters of the SGs used in the test are presented in Table 1.

Figure 9 shows a general block diagram of an autonomous ship power plant system during the parallel operation of two D-G sets implemented in the Sim Power System program of the Matlab-Simulink environment.

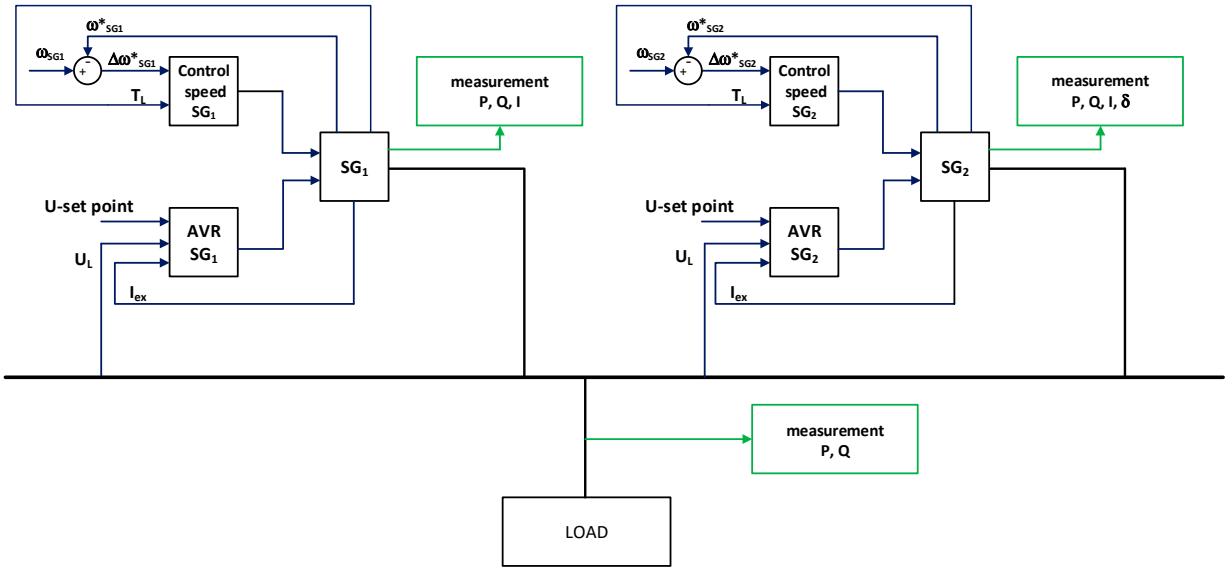

Figure 9. General block diagram of the parallel operation of two generators (SG_1 and SG_2) implemented in the Sim Power System program of the Matlab-Simulink environment.

Each generator (SG_1 and SG_2 blocks) has a rotational speed regulator (Control Speed SG1, Control Speed SG2) and a voltage regulator (Control Excitation SG1, Control Excitation SG2). SG_1 and SG_2 operate in parallel on a common load. Loss of excitation occurs as a

result of asymmetry in the excitation circuits of the generators. The initial asymmetry was simulated in SG_2 through a change in the U-set point.

Figure 10 presents the waveforms of the values of apparent currents I_1 and I_2 operating in parallel (SG_1 and SG_2).

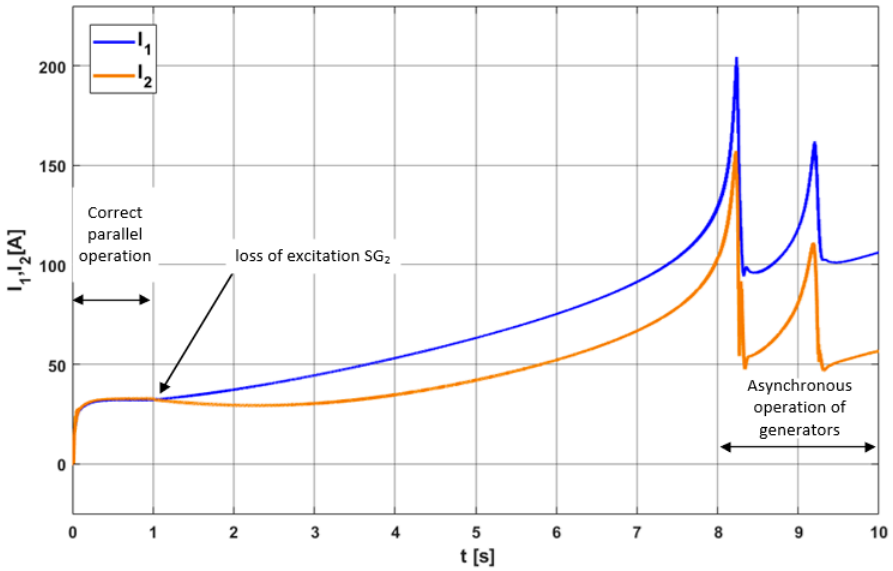

Figure 10. Values of the apparent currents I_1 and I_2 operating in parallel (SG_1 and SG_2).

The current I_1 of SG_1 (of the undamaged generator) increases faster than the current I_2 of SG_2. This is caused by the fact that the reactive current of SG_1 is the sum of the reactive current of SG_2 and the reactive current of the load (Figure 4). The results of the simulation tests confirm the previously conducted analysis (Figure 5).

Figure 11 presents the change in the load angle δ_2 of SG_2. The loss of excitation in SG_2 occurs when $\delta_2 = 1.57$ rad ($\delta_2 = 90^\circ$).

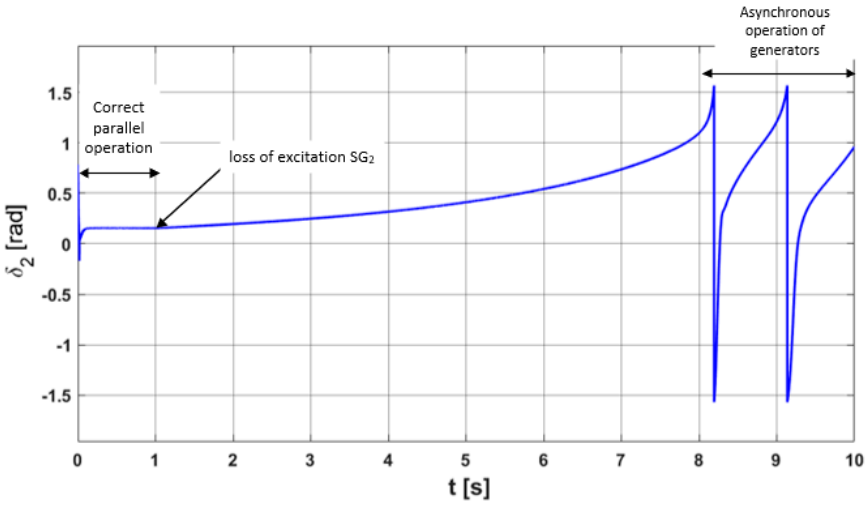

Figure 11. The waveform of the load angle δ_2 with the loss of excitation for SG_2.

With the loss of excitation in the SG_2 generator, the energy of the whole ship's power system (thanks to the existence of the regulators in each generator set (SG_1 and SG_2)) begins to oscillate. This is a characteristic feature in the asynchronous operation of synchronous generators. The results of the examinations confirm the previous analysis (Figure 7).

Figure 12 presents the waveforms of the active and reactive power of the load (P_L, Q_L), as well as the active and reactive power of SG_1 (P_{SG1}, Q_{SG1}) and SG_2 (P_{SG2}, Q_{SG2}).

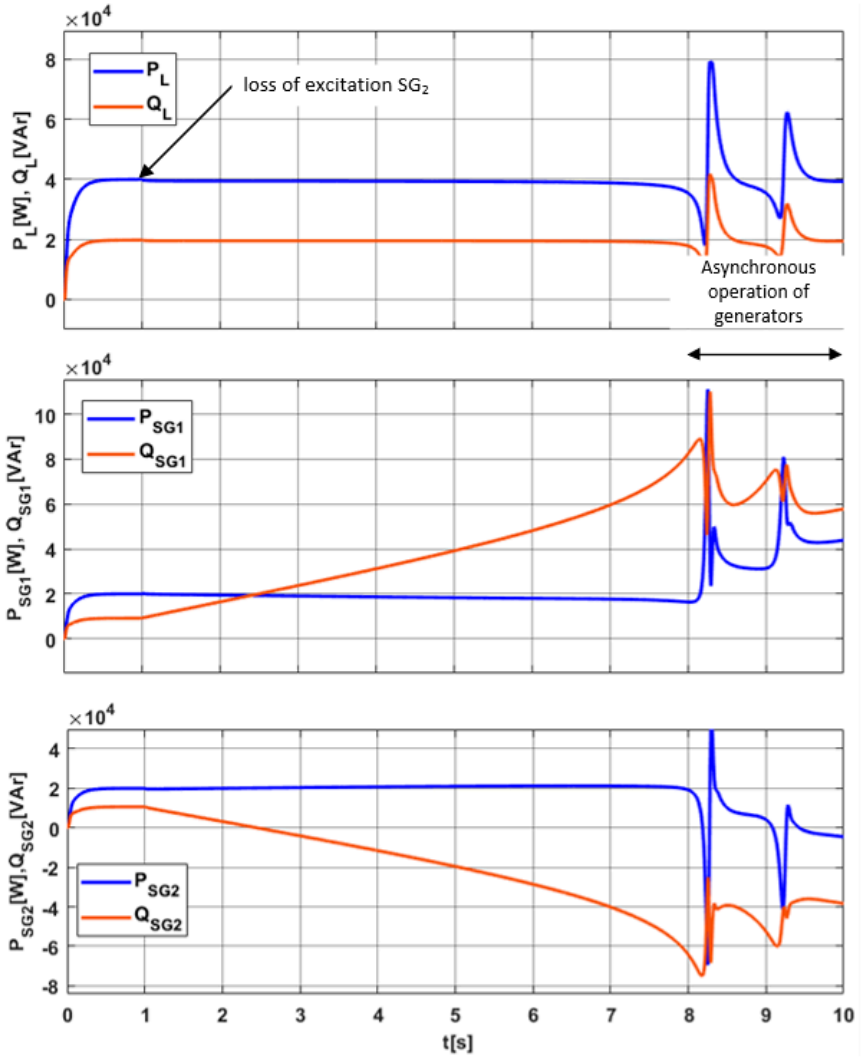

Figure 12. Energy characteristics of the active and reactive power of the load (P_L, Q_L), as well as the active and reactive power for SG_1 (P_{SG1}, Q_{SG1}) and SG_2 (P_{SG2}, Q_{SG2}).

The active and reactive power (P_L, Q_L) is maintained at a constant level until the loss of excitation (generator SG_2) and the transition of the generating sets of the ship's power system into an oscillating state.

SG_2 and SG_1 are symmetrically loaded with active power until the generators are switched to asynchronous operation. The reactive power (Q_{SG1}) increases in order to meet the demand for inductive reactive power of the load and the second generator. The reactive power (Q_{SG2}) decreases to zero and then changes sign.

In order to present the energy dependencies in the autonomous ship power plant system in the parallel operation of the two generating sets in a more accurate way, simulations were carried out with only the active load ($Q_L = 0$). Such a mode of operation corresponds to the characteristics for $P = 0$ in Figure 2—when the initial state of operation for the sets is positioned at point C.

Figure 13 presents the simulation results in this operating mode. The reactive power flow between generators occurs as a result of the positive feedback in the system when the SG_1 is a source of capacitive reactive power for SG_2.

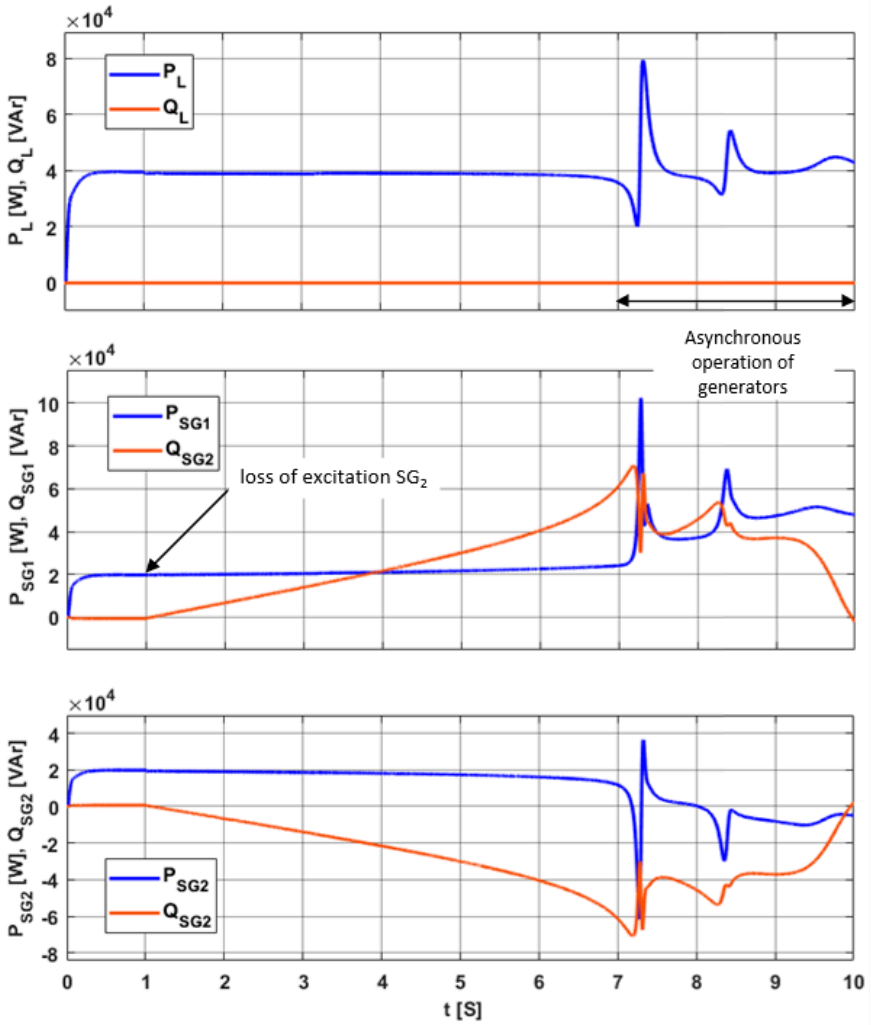

Figure 13. Energy characteristics of the active and reactive power of the load (P_L, Q_L), as well as the active and reactive power for SG_1 (P_{SG1}, Q_{SG1}) and SG_2 (P_{SG2}, Q_{SG2}) with an active load.

4. Experimental Results

The tests on the parallel operation of the D-G_1 and D-G_2 sets were conducted on a laboratory stand, the schematic diagram of which is presented in Figure 14. The main elements of the stand were:

- SG_1, SG_2—synchronous generators (type: ELMOR GCf74) with the parameters presented in Table 1;
- CM_1, CM_2—squirrel cage motors of the generators—ELMOR MSSfc200L4;
- $CONV_1$, $CONV_2$—power converters of CM_1 and CM_2;
- AVR—automatic voltage regulator for the generators—ANCIAC 80;
- M1—energy and power quality meter—TEAMWARE-WALLY_A/A^3 (measurement: I_1, P_1, Q_1);
- M2—energy and power quality meter—SONEL-PQM700 (measurement: I_2, P_2, Q_2);
- RL—load on the generating sets (12 kW, 4.8 kVAr).

Figures 15 and 16 present the view of the laboratory stand.

The tests were performed after the synchronization of the generating sets and the distribution of active and reactive powers in a symmetrical way (k = 0.5; Equation (4)). The RL loads of the generating sets were: active power load P_L = 12.1 kW and reactive power load Q_L = 4.85 kVAr.

The time courses of the currents, as well as the active and reactive power, were recorded with the use of electric power quality meters M_1 and M_2 (the sampling period

was set to 1 s; the maximum sampling frequency of meter M_2 was 1 Hz). The voltage point for the voltage regulator of generator SG_2 was set to a minimum value in order to simulate the loss of excitation. Figures 17 and 18 show the waveforms of the reactive power (Q_1 and Q_2) and active power (P_1 i P_2) emitted by the generating sets that were operating in parallel.

Until t = 15 s, generating set SG_2 worked alone. At t = 15 s, set SG_1 was active. Then, at t = 39 s, there was a synchronization and symmetrical power distribution. The sets worked symmetrically until t = 80 s. Then, there was a partial loss of SG2′s excitation. The inductive reactive power (Q_2) decreased to zero, and then it started to increase with a changed sign (Q_2—capacitive; Figures 3b and 8).

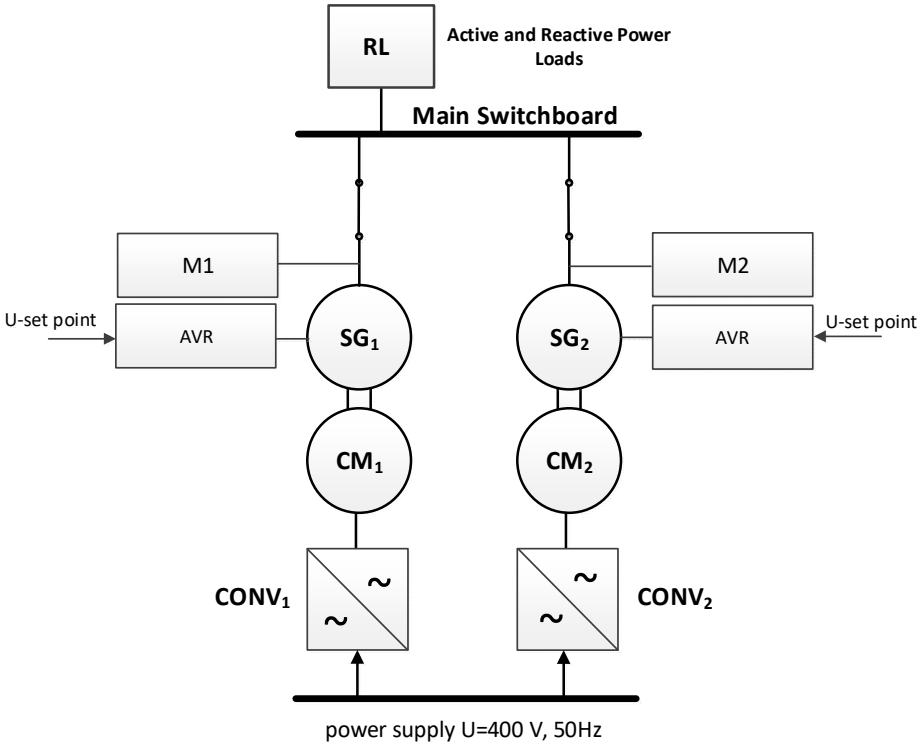

Figure 14. Schematic diagram of the laboratory stand.

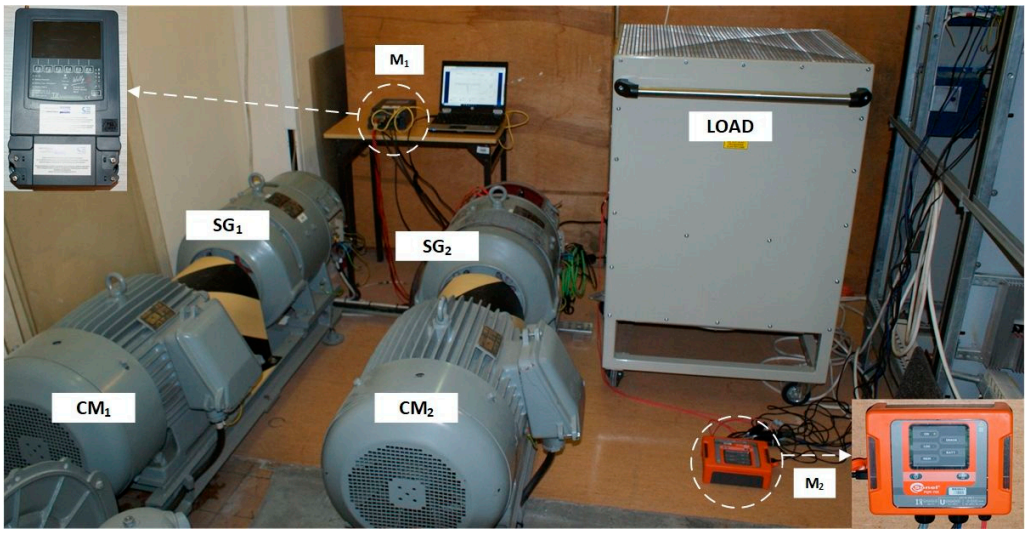

Figure 15. Laboratory stand: generating sets: CM_1—SG_1 and CM_2—SG_2, RL load, and power quality meters: M_1 and M_2 (for the parameters of SG_1 and SG_2).

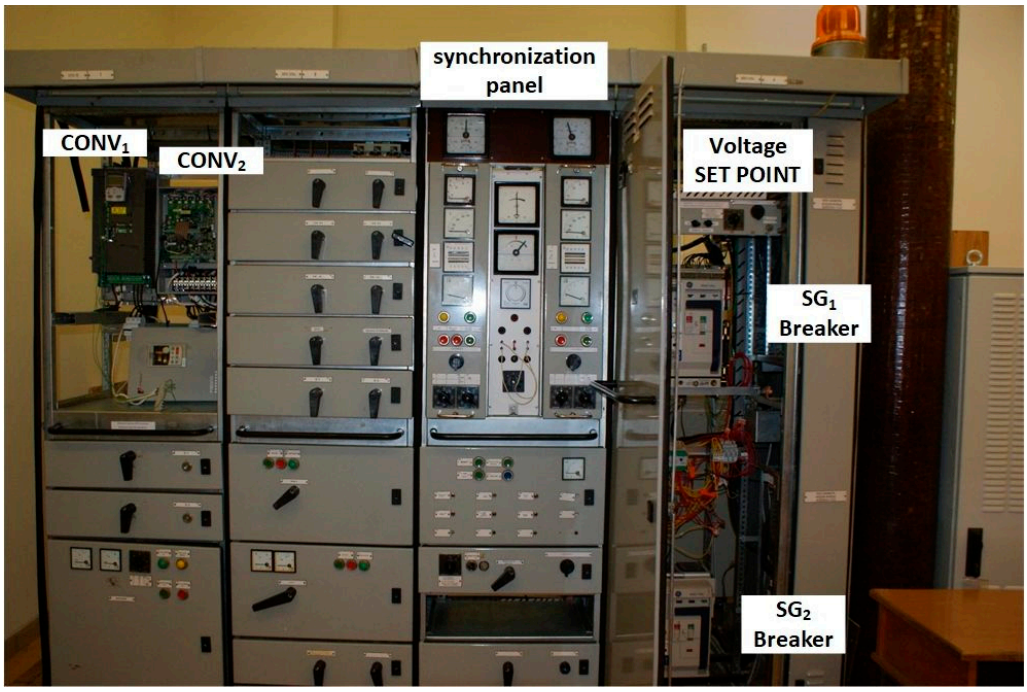

Figure 16. Laboratory stand: main switchboard; $CONV_1$ and $CONV_2$—converters supplying the electric motors (CM_1, CM_2).

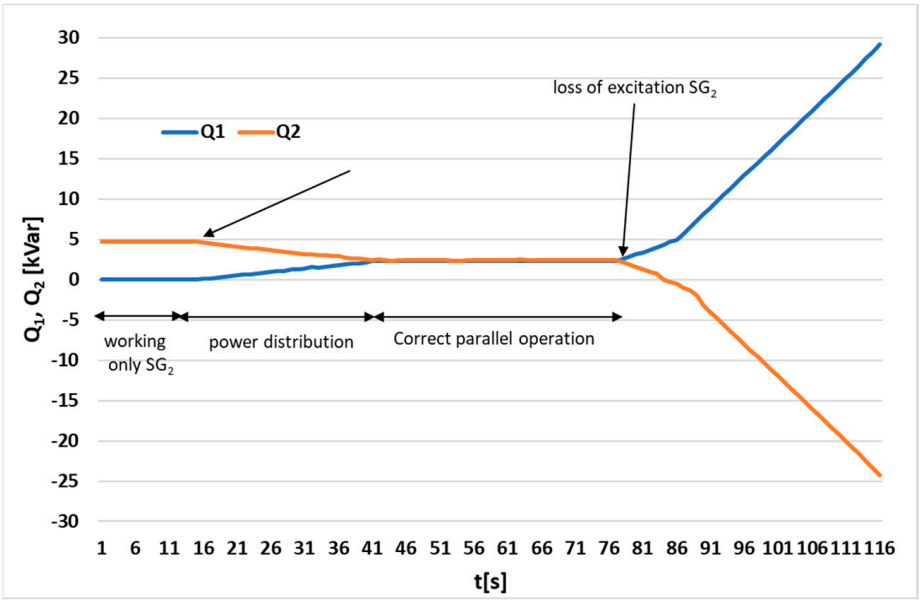

Figure 17. Waveforms of the reactive power (Q_1 and Q_2) obtained during the laboratory tests.

Figure 19 presents the effective values of the apparent currents for both generators. At the moment of partial loss of excitation for SG_2, the current I_2 began to temporarily decrease (until the value of the reactive current component was zero), and then increased—it significantly exceeded the nominal current I_N. At the same time, the current I_1 start to increase (faster), exceeding the I_N value.

In order to protect the generators against damage, the tests were interrupted when the I_1 current was exceeded by approximately $1.5 \times I_N$. It was not possible to ensure the asymmetrical operation of the generators.

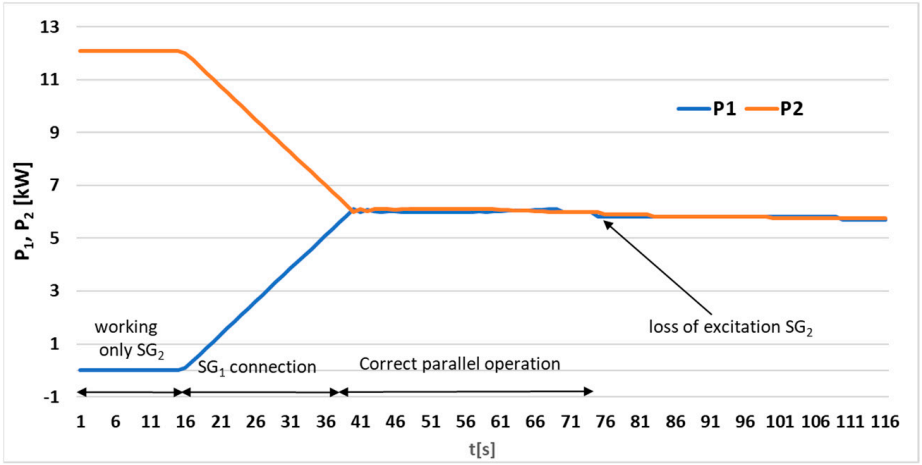

Figure 18. Waveforms of the active power (P_1 and P_2) obtained during the laboratory tests.

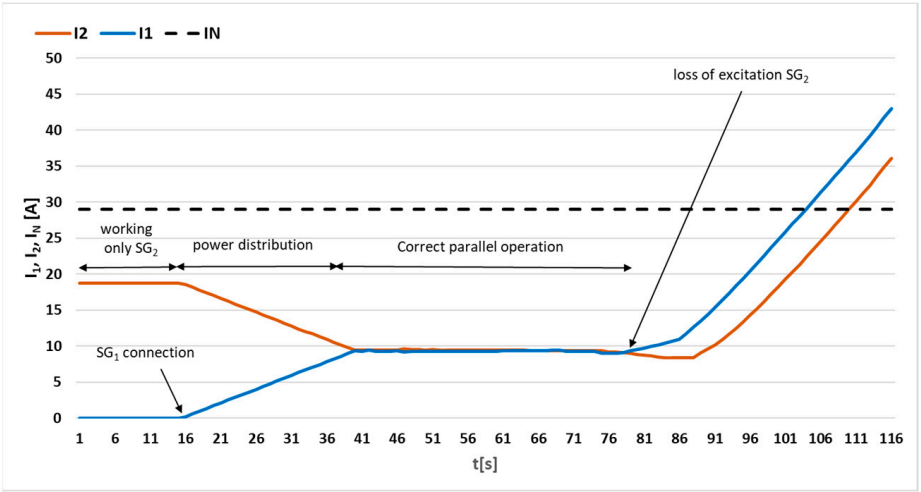

Figure 19. Time waveforms of currents I_1 and I_2 obtained during the laboratory tests.

5. Discussion

Two aspects that explain the importance of this problem can be highlighted here. The first concerns ensuring the safety of the ship. Disturbances in the parallel operation of generators can lead to failures of the power system, disconnection of the ship from the power supply, loss of controllability, and catastrophes. Secondly, the economic considerations connected with the operation of each ship are important. Power that is generated with a low quality leads to increased fuel consumption, longer duration of the cruise, and additional costs connected with the repair of equipment. It should be considered that, in the majority of cases, synchronous generators are powered by diesel combustion engines. This means that the process of ensuring safe parallel operation must be considered in conjunction with these diesel combustion engines [8].

The results of the laboratory tests were confirmed by the analytical and simulation examinations. Because of the specificity of the autonomous ship grid, when a generating set operates in parallel, an LOE in one generator has a decisive impact on the operation of the set. The tests showed that the value of the inductive reactive power generated by an efficient generator covers the demand for the inductive reactive power of the receiver and the capacitive reactive power of the generator that had lost the excitation. The current of an efficient generator increases faster than the current of a damaged generator. The reactive component of the current in an efficient generator is the sum of the reactive component of the current in the damaged generator and the reactive component of the load current. When the load angle ($\delta > 90^{\circ}$) of a generator that has lost its excitation is exceeded, the power

system switches to the asymmetric operation of both generators (oscillations of power and currents). The active power transmitted by both generating sets remains constant until the oscillation.

The simulation tests with an active load ($Q_L = 0$) showed that when the excitation of one of the operating generators was lost, there was a significant flow of reactive power between the generators (Figure 17).

This research confirms that in the event of activation of protection (instantaneous short-circuit protection), the efficient generator may first be disconnected from the system. A generator that has lost its excitation will be disconnected from the system by the undervoltage protection, and there will be a blackout.

6. Conclusions

To the best of the authors' knowledge, the problem of loss of excitation during the parallel operation of two generators in (autonomous) ship power grids was tested for the first time in this article. The instability of the power system is treated as the existence of positive feedback in this system. This leads to the loss of synchronization in the cooperation between the two generators. Analytical examinations have shown that in the case of the loss of stability conditions (asymmetry of voltage control systems) in sets operating in parallel, when one generator loses its excitation, the second generator takes over the reactive load of the entire set.

These research results show that in autonomous ship grids, unlike with the operation of generating sets with a rigid grid, there are mutual influences from the electromagnetic and energy processes in all generators that are operating in parallel.

The research presented in this article showed that, in the event of LOE occurrence in one of the generators, the current will increase in both generators. However, the current in an undamaged generator will be higher than that in a damaged one because the reactive current is the sum of the reactive current of the generator where the LOE occurred and the reactive current of the load. Therefore, the currently used protections (required by the rules and regulations for the classification of ships)—in this case, overload protection—will first operate on an undamaged generator, thus turning this generator off. It should also be noted that the generator overload protection used on ships usually has a time delay of approximately 20 s. During this time, the current can significantly exceed its nominal value and, in extreme cases, the generators may work asynchronously. After disconnection of the undamaged generator, the voltage protection will switch off the damaged one. As a consequence, this may lead to a serious threat to the safety of the ship. The only solution to this problem is the use of a protective device against excitation loss (e.g., the SELCO—Excitation Loss Relay T2100 [24]).

The analytical and simulation tests, as well as the experimental results presented in this article, prove the necessity of introducing mandatory global regulations that will oblige marine classification societies to adjust the protections of ship generators to account for loss of excitation. Moreover, it is necessary to introduce similar protections in onshore autonomous power plants.

Author Contributions: Conceptualization, D.T., S.G.-G., and M.S.; methodology, D.T., S.G.-G., and M.S.; software, D.T. and S.G.-G.; validation, D.T., S.G.-G., and M.S.; formal analysis, D.T. and S.G.-G.; investigation, D.T., S.G.-G., and M.S.; resources, D.T., S.G.-G., and M.S.; data curation, D.T., S.G.-G., and M.S.; writing—original draft preparation, D.T. and S.G.-G.; writing—review and editing, D.T., S.G.-G., and M.S.; visualization, D.T., S.G.-G., and M.S.; supervision, D.T. and S.G.-G.; project administration, D.T. and S.G.-G.; funding acquisition, D.T., S.G.-G., and M.S. All authors have read and agreed to the published version of the manuscript.

Funding: This research received no external funding.

Institutional Review Board Statement: Not applicable.

Informed Consent Statement: Not applicable.

Data Availability Statement: Not applicable.

Conflicts of Interest: The authors declare no conflict of interest.

References

1. Yasakov, G.S. *Ship Electric Power Systems*; Part 1—S.-Pb; N. G. Kuznetsov Naval Academy: Saint Petersburg, Russia, 1999.
2. Śmierzchalski, R. *Automation of the Ship's Power System*; Graphics Center: Gryf Gdańsk, Poland, 2004; ISBN 83-921110-5-2.
3. Tarnapowicz, D. Load Analysis of a Ship Generating Sets During the Maneuvers of the Vessel. In Proceedings of the 59th International Conference of Machine Design Departments, Demanovska Dolina, Slovakia, 11–14 September 2018. [CrossRef]
4. Al-Falahi, M.D.A.; Tarasiuk, T.; Jayasinghe, S.G.; Jin, Z.; Enshaei, H.; Guerrero, J.M. AC Ship Microgrids: Control and Power Management Optimization. *Energies* **2018**, *11*, 1458. [CrossRef]
5. Shifa, F.A. A Discussion on the Optimal Selection of Parameters for Determination of Engine Dimensions in a Diesel Electric (DE) Power Station. In Proceedings of the International Electrical Engineering Congress, Pattaya, Thailand, 8–10 March 2017.
6. Ochoa, D.; Martinez, S. Proposals for Enhancing Frequency Control in Weak and Isolated Power Systems: Application to the Wind-Diesel Power System of San Cristobal Island-Ecuador. *Energies* **2018**, *11*, 910. [CrossRef]
7. Moon, H.; Kim, Y.J.; Chang, J.W.; Moon, S. Decentralised Active Power Control Strategy for Real-Time Power Balance in an Isolated Microgrid with an Energy Storage System and Diesel Generators. *Energies* **2019**, *12*, 511. [CrossRef]
8. Savenko, A.E.; Golubev, A.N. *Exchange Power Fluctuations in Shipboard Electrical Complexes*; Federal State-Financed Educational Institution of Higher Professional Education Ivanovo State Power Engineering University: Ivanovo, Russia, 2016.
9. IEC. *IEC 60092-202: Electrical Installations in Ships–Part 202: System Design–Protection*; IEC: Geneva, Switzerland, 2016.
10. Lloyd's Register. *Rules and Regulations for the Classification of Ships*; Part 6 Control, Electrical, Refrigeration and Fire, Chapter 2 Electrical Engineering, Section 6 System Design—Protection, 6.8 Protection of Generators; LR: London, UK, 2020.
11. Bureau Veritas. *Rules for the Classification of Steel Ships*; Part C Machinery, Electricity, Automation and Fire Protection. Chapter 2 Electrical Installations Section 3 System Design 7 Electrical Protection 7.8 Protection of Generators; BV: Paris, France, 2021.
12. PRS Classification Rules Part VIII. In *Electrical Installations and Control Systems*; PRS: Gdańsk, Poland, 2007.
13. DNV GL. *Classification Rules*; Part 4 Systems and Components Chapter 8 Electrical Installations; DNV GL: Oslo, Norway, 2020.
14. Hu, J.-y.; Liang, Y.-p.; Chen, J.; Huang, H. Simulation Analysis for Asynchronous Operation Capacity of Turbogenerator under Excitation-Loss. In Proceedings of the 2011 6th International Forum on Strategic Technology, Harbin, China, 22–24 August 2011; IEEE: Piscataway Township, NJ, USA, 2011.
15. Gazen, Y.N.; Zarnott, A.B.; Peres de Morais, A.; Cardoso, G.; Oliveira, A. New setting of loss of excitation protection in P-Q plan in order to maximize the operation area of the capacity curve of the synchronous machine. In Proceedings of the 2014 49th International Universities Power Engineering Conference (UPEC), Cluj-Napoca, Romania, 2–5 September 2014; IEEE: Piscataway Township, NJ, USA, 2017.
16. López, M.D.; Platero, C.A.; Mayor, P.L.; Granizo, R. Review of loss of excitation protection setting and coordination to the generator capacity curve. In Proceedings of the 2017 IEEE International Conference on Environment and Electrical Engineering and 2017 IEEE Industrial and Commercial Power Systems Europe (EEEIC/I&CPS Europe), Milan, Italy, 6–9 June 2017; IEEE: Piscataway Township, NJ, USA, 2017.
17. Gallas, M.; Morais, A.P.; Marchesan, A.C.; Cardoso, G.; Costa, G.B. A Comparative Analysis of Loss of Excitation Protection Methods for Synchronous Generators. In Proceedings of the 2017 IEEE International Conference on Environment and Electrical Engineering and 2017 IEEE Industrial and Commercial Power Systems Europe (EEEIC/I&CPS Europe), Milan, Italy, 6–9 June 2017; IEEE: Piscataway Township, NJ, USA, 2017.
18. Coelho, A.L.M.; Carrer, C.E.B.; Guerrero, C.A.V.; Silveira, P.M. Loss-of-excitation protection and underexcitation controls correlation for synchronous generators in a real time digital simulator. In Proceedings of the 2014 IEEE Industry Application Society Annual Meeting, Vancouver, BC, Canada, 5–9 October 2014; IEEE: Piscataway Township, NJ, USA, 2014.
19. Li, L.; Caixin, S.; Daohuai, M. Study on the Excitation Protection and Control of Synchronous Generator Based on the δ and s. In Proceedings of the 2005 IEEE/PES Transmission & Distribution Conference & Exposition: Asia and Pacific, Dalian, China, 8 December 2014; IEEE: Piscataway Township, NJ, USA, 2014.
20. Kentli, F.; Birbir, Y.; Onat, N. Examination of the stability limit on the synchronous machine depending on the excitation current wave shape. In Proceedings of the IEMDC 2001 IEEE International Electric Machines and Drives Conference, Cambridge, MA, USA, 17–20 June 2001; IEEE: Piscataway Township, NJ, USA, 2001.
21. Wang, X.; Han, M.; Teshager, B.G. A Novel Method to Analyze the Reactive Power Characteristic of Doubly Fed Adjustable-Speed Pumped Storage Unit. In Proceedings of the 2018 International Conference on Power System Technology (POWERCON), Guangzhou, China, 6–8 November 2018; IEEE: Piscataway Township, NJ, USA, 2018.
22. Tokarev, L.N. *Mathematical Description, Calculation and Modeling of Physical Processes in Ship Power Plants*; Shipbuilding: Leningrad, Russia, 1980; ISSN 0039-4580.
23. German-Galkin, S.; Tarnapowicz, D.; Matuszak, Z.; Jaskiewicz, M. Optimization to Limit the Effects of Underloaded Generator Sets in Stand-Alone Hybrid Ship Grids. *Energies* **2020**, *13*, 708. [CrossRef]
24. SELCO ApS. Available online: http://www.selco.com/selco2016/wp-content/uploads/2017/02/T2100-Datasheet_2.pdf (accessed on 1 April 2021).